Influence of magnetic nanoparticles on cells of Ehrlich ascites carcinoma

Cite as: AIP Advances **11**, 015019 (2021); https://doi.org/10.1063/9.0000165
Submitted: 27 October 2020 • Accepted: 24 November 2020 • Published Online: 07 January 2021

S. V. Stolyar, O. V. Kryukova, R. N. Yaroslavtsev, et al.

Influence of magnetic nanoparticles on cells of Ehrlich ascites carcinoma

Cite as: AIP Advances 11, 015019 (2021); doi: 10.1063/9.0000165
Presented: 6 November 2020 • Submitted: 27 October 2020 •
Accepted: 24 November 2020 • Published Online: 7 January 2021

S. V. Stolyar,[1,a)] O. V. Kryukova,[1] R. N. Yaroslavtsev,[1] O. A. Bayukov,[2] Yu. V. Knyazev,[2] Yu. V. Gerasimova,[2] V. F. Pyankov,[1] N. V. Latyshev,[1] and N. P. Shestakov[2]

AFFILIATIONS

[1]Krasnoyarsk Scientific Center, Federal Research Center KSC SB RAS, 660036 Krasnoyarsk, Russia
[2]Kirensky Institute of Physics, Federal Research Center KSC SB RAS, 660036 Krasnoyarsk, Russia

Note: This paper was presented at the 65th Annual Conference on Magnetism and Magnetic Materials.
[a)]**Author to whom correspondence should be addressed:** stol@iph.krasn.ru

ABSTRACT

The effect of magnetic nanoparticles coated with arabinogalactan on the viability of Ehrlich ascites carcinoma (EAC) cells was studied. The nanoparticles were studied by transmission electron microscopy, Mössbauer spectroscopy, IR spectroscopy, and ferromagnetic resonance. A correlation between the proportion of dead EAC cells in suspension and the intensity of the EPR signal of dinitrosyl iron complexes was found. This result may be due to the presence of NO molecules.

I. INTRODUCTION

Currently, nanoparticles (including non-magnetic) are attracting special attention for use in tumor immunotherapy. Nanoparticles can affect the phagocytic activity of macrophages, the yield of nitric oxide (NO) and reactive oxygen species.[1] Nitric oxide is capable of both stimulating the growth of tumor cells and exerting a cytotoxic effect.[2] NO in cells and tissues can form paramagnetic dinitrosyl iron complexes (DNIC). Polysaccharide-coated magnetite nanoparticles have shown a promising antitumor effect by activating tumor-associated macrophages from a tumor-promoting phenotype to a tumor-suppressing phenotype.[3] The authors of Ref. 4 have demonstrated that magnetite nanoparticles are more effective than hematite nanoparticles in polarizing macrophages and suppressing tumors. Among the magnetic nanoparticles involved in the metabolism of living organisms, ferrihydrite with the nominal formula $Fe_2O_3{\cdot}nH_2O$ plays a special role. It is formed in the nucleus of the ferritin protein complex, which is a capsule of the protein apoferritin and serves as the storage of iron in the body. The size of ferrihydrite nanoparticles lies in a narrow range from 1 to 8 nm. With an increase in the particle size, the transformation $Fe_2O_3{\cdot}nH_2O \rightarrow$ hematite occurs.[5] Ferrihydrite is an antiferromagnet with a Néel temperature of ≈ 350 K.[6] Structure, resonance properties and biomedical applications of ferrihydrite nanoparticles were studied in Ref. 7–13.

This work aims to synthesize and study the magnetic properties of ferrihydrite nanoparticles coated with the natural polysaccharide arabinogalactan, as well as to study the possible effect of ferrihydrite nanoparticles on the suppression of Ehrlich ascites carcinoma (EAC) tumor.

II. EXPERIMENTAL

Nanoparticles were prepared by precipitation with an ammonium hydroxide solution under conditions of ultrasonic cavitation. To a solution containing 0.4% iron nitrate $Fe(NO_3)_3$ and 0.5% arabinogalactan, a solution of ammonium hydroxide NH_4OH (2.5% vol) was added dropwise. During the synthesis, the solution was treated with ultrasound (50 W/cm^2, 22 kHz).

Structural studies were performed using a Hitachi HT7700 transmission electron microscope. The Mössbauer spectra were measured on an MS-1104Em spectrometer with a source of 57Co(Cr) on powder samples with a thickness of 5–10 mg/cm^2 on the basis of the natural iron content. The FTIR absorption spectra were obtained on a Vertex 80 spectrometer (Bruker). Resonant absorption curves at a frequency of 9.4 GHz were recorded on an Elexsys E580 spectrometer (Bruker) at temperatures from 120 to 360 K.

We used the Ehrlich's ascites carcinoma (EAC). This is a popular inoculated undifferentiated cancer model for studying various

aspects of tumor destruction in mice due to the high sensitivity of EAC to external influences.[14]

EAC cells were collected from the peritoneal cavity of mice after 10 days of the tumor inoculation. Further, the suspension of tumor cells was divided into groups - control and experimental. The cells of the experimental groups were incubated *in vitro* with magnetic nanoparticles of ferrihydrite coated with arabinogalactan for 60 min at 34 °C. The EAC cells viability was determined using a light microscope, which is part of the unique scientific unit "Complex of equipment for regulated cultivation of isolated organs". To assess the viability of EAC cells, staining with a 1% trypan blue solution was performed. For magnetic resonance studies, the following samples were prepared: EAC suspension (control), ascites plasma, and EAC and MNP suspension. EPR spectra were recorded at a temperature of 85 K.

III. RESULTS AND DISCUSSION

The results of high-resolution transmission electron microscopy of iron oxide nanoparticles are shown in Figure 1. The average particle size is ~ 2 nm. According to the diffraction image, the nanoparticles are ferrihydrite.

Figure 2a shows the Mössbauer spectrum of nanoparticles measured at room temperature. The spectrum is a quadrupole doublet characteristic of particles in the superparamagnetic state. An analysis of the distribution of quadrupole splitting leads to the conclusion that there are at least three nonequivalent iron positions with an octahedral environment and one position with a tetrahedral environment of the ligands. The result of the interpretation of the Mössbauer spectra is summarized in Table 1. The parameters of the model spectra are in good agreement with the results obtained earlier for ferrihydrite powders.[8,15,16] Figure 2b shows the Mössbauer spectrum of nanoparticles measured at a temperature of 4K. The number of detected sextets (Table 1) coincides with the results of the analysis of the Mössbauer spectrum of ferrihydrite at 300 K. The spectrum parameters agree with the parameters of the Mössbauer spectra obtained from ferrihydrites of natural and artificial origin.[17]

Note that these nanoparticles contain iron in tetrahedral coordination, in contrast to biogenic and synthetic samples that we studied earlier.[8,15,16] This can be attributed to the use of cavitation ultrasonic treatment, which stimulates the release of iron ions from the octahedral environment.

The IR absorption spectra of arabinogalactan and nanoparticles coated with arabinogalactan are shown in Figure 3.

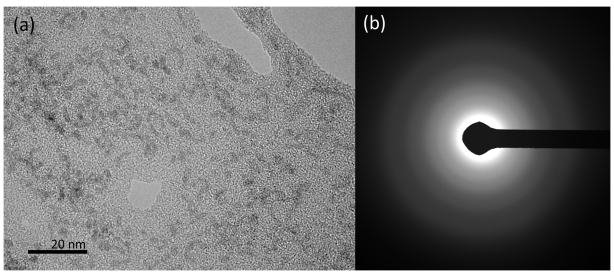

FIG. 1. TEM-image (a) and diffraction pattern (b) of ferrihydrite nanoparticles coated with arabinogalactan.

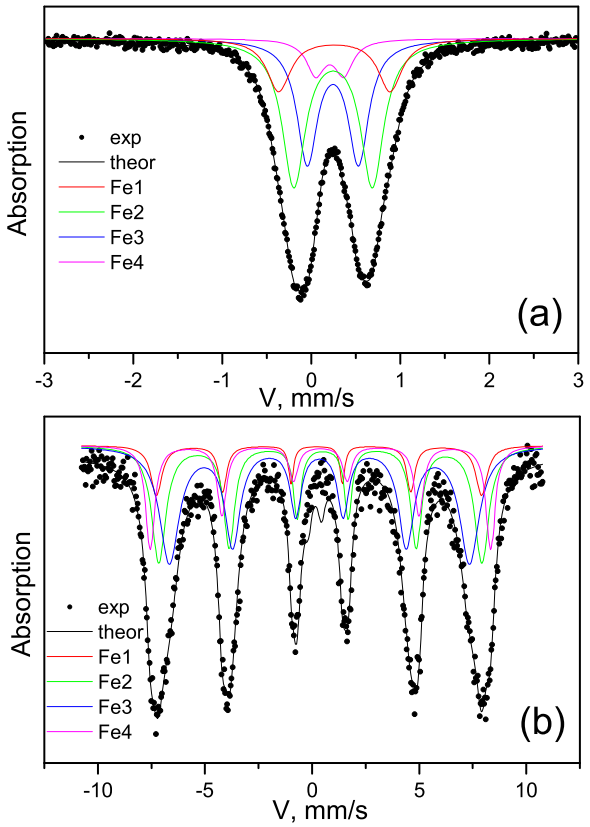

FIG 2. Mössbauer spectra of ferrihydrite nanoparticles measured at 300 K (a) and 4 K (b).

The spectrum of arabinogalactan exhibits a broad band in the range of 2900-3400 cm-1, in which the absorption bands of O–H bonds (3400 cm^{-1}) and CH, CH_3-, CH_2- (~2900 cm^{-1}) carbohydrate units overlap. The vibration of 1640 cm^{-1} corresponds to the vibrations of the carbonyl group; 1370 cm^{-1} is the deformation vibrations of the diol alcohol groups δ-OH. In the region of 1200-1000 cm^{-1}, we observe some bands belonging to stretching vibrations of the

TABLE 1. Mössbauer parameters.

	ChemS	HFF	QuadrS	WidthS	AreaS	Position
300 K	0.31	...	0.32	0.25	0.08	Fe(4)
	0.35	...	0.58	0.28	0.32	Fe1(6)
	0.35	...	0.88	0.31	0.44	Fe2(6)
	0.37	...	1.25	0.32	0.16	Fe3(6)
4 K	0.378	473	0.213	0.211	0.10	Fe(4)
	0.549	470	−0.227	0.368	0.31	Fe1(6)
	0.453	436	0.003	0.543	0.42	Fe2(6)
	0.498	495	0.001	0.508	0.17	Fe3(6)

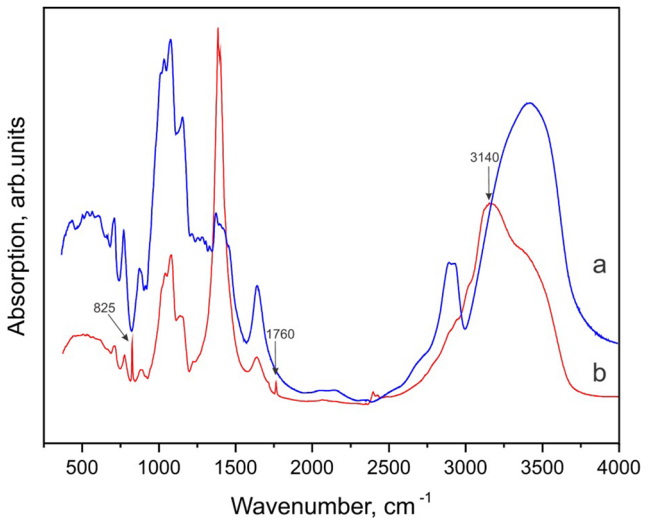

FIG. 3. FTIR spectra at room temperature: a) arabinogalactan, b) ferrihydrite nanoparticles coated with arabinogalactan.

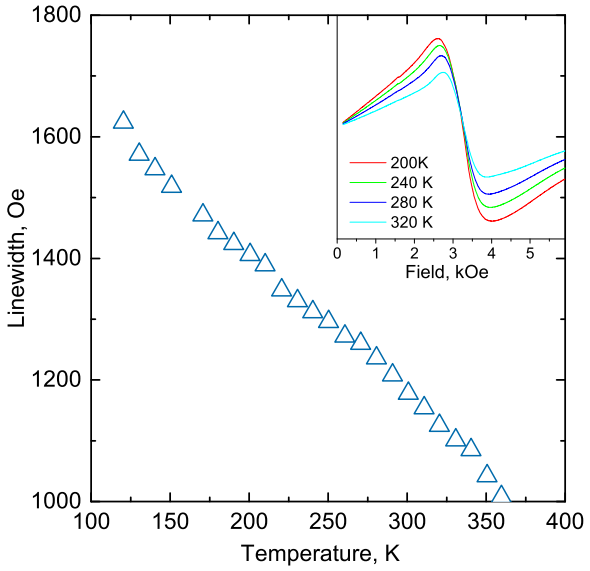

FIG. 4. Temperature dependence of the ferromagnetic resonance linewidth of ferrihydrite nanoparticles. The inset shows the ferromagnetic resonance spectra.

C-O bond of the pyranose and furanose rings, as well as bending vibrations of the cycles (714, 775, 882 cm^{-1}).

The main difference between the IR spectrum of nanoparticles and the IR spectrum of arabinogalactan is the absence of an absorption band in the region of 2900 cm^{-1}. In the spectrum of nanoparticles, the maximum at a frequency of 3140 cm^{-1} belongs to the ≡C-H bond.

The most intense band in the spectrum of nanoparticles belongs to the bending vibrations of the diol alcohol groups δ OH (1385 cm^{-1}). The band 1000–1200 cm^{-1} has a lower intensity than in the spectrum of pure arabinogalactan. New absorption bands appeared at frequencies of 1760 and 825 cm^{-1}. In the IR spectrum of the nanoparticles, the 1760 cm^{-1} band refers to the stretching vibrations of the C=O bond of the ionized carboxyl group formed as a result of iron reduction. The 825 cm^{-1} band is related to the C–H bond.

The inset in Fig. 4 shows the ferromagnetic resonance curves measured in the temperature range from 120 to 360 K. The absorption intensity in this temperature range decreases linearly, indicating that the nanoparticles are in an unblocked, superparamagnetic state. The values of the resonance fields $H_R(T)$ monotonically increases from 3.32 kOe to 3.38 kOe in the used temperature range, reaching saturation at T≈350K. Figure 4 shows the temperature dependence of the ferromagnetic resonance linewidth ΔH(T) of ferrihydrite nanoparticles. The experimental curve ΔH(T) at T ≥ 300 K changes the functional dependence (the derivative passes through a maximum). The observed features in the dependencies $H_R(T)$ and ΔH(T) of ferrihydrite nanoparticles are possibly due to the Néel temperature of ferrihydrite.[6]

Figure 5(a) shows a characteristic curve of the resonant absorption of an EAC suspension. Absorption due to transferrin, cytochrome molecules, ceruloplasmin, and also Mo^{2+}-containing molecules are observed. Absorbances with a g-factor of 2.01-2.04, indicated in the figure by 4, are reliably recorded. These absorption

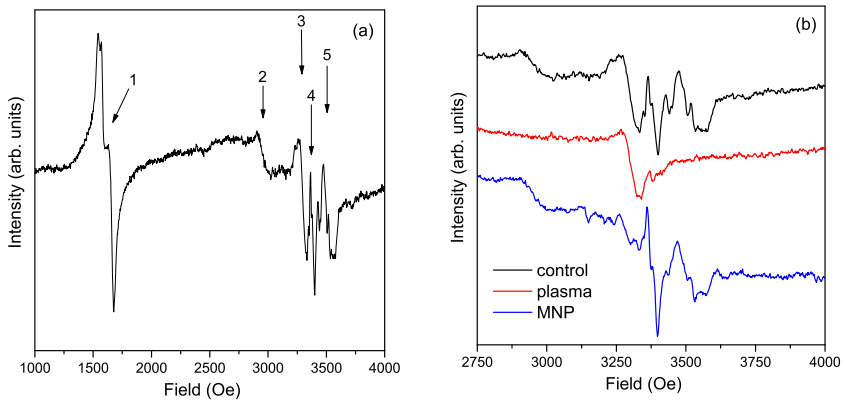

FIG. 5. (a) EPR spectrum of the EAC. Peaks: 1- transferrin; 2- cytochromes; 3- ceruloplasmin; 4-DNIC; 5-Mo^{2+}-containing molecules. (b) EPR spectra of samples - control of the EAC, plasma, and EAC + MNP.

peaks are due to the presence of DNIC, which include endogenous Fe and thiol (sulfur-containing) groups.[18]

Figure 5(b) shows the high-field sections of three resonance curves: isolated tumor (control), EAC cells cultured with used nanoparticles and plasma obtained after centrifugation of the EAC suspension.

A comparison of these curves indicates that ceruloplasmin (and transferrin) are exclusively in the plasma, and the presence of dinitrosyl iron complexes is associated with tumor cells and peritoneal macrophages present in the EAC suspension. Figure 5(b) shows that the cultivation of a suspension of EAC with nanoparticles leads to a noticeable decrease in the signal from ceruloplasmin and an increase in the signal from dinitrosyl complexes.

The proportion of dead cells with the addition of ferrihydrite nanoparticles (17.5%) was higher than in the control (11.5%) and with the addition of arabinogalactan (10.7%). With an increase in the intensity of the DNIC signal, i.e. an increase in NO concentration, the proportion of dead cells increases. A unique feature of EAC cells is that they are capable of producing nitric oxide, which is associated with their defense mechanisms from the immune system.[2,19,20]

Possibly, in our experiments, the main source of NO regulating the number of tumor cells is peritoneal macrophages present in the EAC tumor cell suspension. The cultivation of ascites with magnetic particles increases the yield of nitric oxide NO [see Fig. 5(b)].[1,2] Higher concentrations of NO and, consequently, reactive nitrogen species (RNS), lead to reactions that cause DNA damage,[20] activation of various transcription factors,[21,22] due to which expression of p53 protein can increase, for example causing apoptosis of cells and their death.

IV. CONCLUSION

Magnetic nanoparticles coated with arabinogalactan have been synthesized by chemical precipitation. According to the results of transmission electron microscopy, Mössbauer spectroscopy and ferromagnetic resonance, it was determined that the synthesized magnetic nanoparticles are ferrihydrite. The increase in the proportion of dead Ehrlich ascites carcinoma cells is due to an increase in the yield of nitric oxide in the cell suspension during cultivation with magnetic nanoparticles.

ACKNOWLEDGMENTS

The electron microscopy and magnetic resonance study was carried out on the equipment of the Krasnoyarsk Territorial Center for Collective Use, Krasnoyarsk Scientific Center, Siberian Branch, Russian Academy of Sciences. This work was supported by the Council of the President of the Russian Federation for State Support of Young Scientists and Leading Scientific Schools (project no. MK-1263.2020.3). The research was funded by RFBR, Krasnoyarsk Territory and Krasnoyarsk Regional Fund of Science, project number 20-42-242902.

DATA AVAILABILITY

The data that support the findings of this study are available from the corresponding author upon reasonable request and available within the article.

REFERENCES

[1] Z. Guo, Y. Liu, H. Zhou, K. Zheng, D. Wang, M. Jia, P. Xu, K. Ma, C. Cui, and L. Wang, Colloids Surfaces B Biointerfaces **184**, 110546 (2019).
[2] A. F. Vanin and A. G. Chetverikov, Biofizika **13**, 608 (1968).
[3] S. Zanganeh, G. Hutter, R. Spitler, O. Lenkov, M. Mahmoudi, A. Shaw, J. S. Pajarinen, H. Nejadnik, S. Goodman, M. Moseley, L. M. Coussens, and H. E. Daldrup-Link, Nat. Nanotechnol. **11**, 986 (2016).
[4] Z. Gu, T. Liu, J. Tang, Y. Yang, H. Song, Z. K. Tuong, J. Fu, and C. Yu, J. Am. Chem. Soc. **141**, 6122 (2019).
[5] T. Hiemstra, Geochim. Cosmochim. Acta **158**, 179 (2015).
[6] M. S. Seehra, V. S. Babu, A. Manivannan, and J. W. Lynn, Phys. Rev. B **61**, 3513 (2000).
[7] A. Punnoose, M. S. Seehra, J. van Tol, and L. C. Brunel, J. Magn. Magn. Mater. **288**, 168 (2005).
[8] S. V. Stolyar, R. N. Yaroslavtsev, R. S. Iskhakov, O. A. Bayukov, D. A. Balaev, A. A. Dubrovskii, A. A. Krasikov, V. P. Ladygina, A. M. Vorotynov, and M. N. Volochaev, Phys. Solid State **59**, 555 (2017).
[9] S. V. Stolyar, D. A. Balaev, V. P. Ladygina, A. I. Pankrats, R. N. Yaroslavtsev, D. A. Velikanov, and R. S. Iskhakov, JETP Lett **111**, 183 (2020).
[10] Y. V. Knyazev, D. A. Balaev, S. V. Stolyar, O. A. Bayukov, R. N. Yaroslavtsev, V. P. Ladygina, D. A. Velikanov, and R. S. Iskhakov, J. Alloys Compd. **851**, 156753 (2021).
[11] C. G. Chilom, N. Sandu, M. Bălăşoiu, R. N. Yaroslavtsev, S. V. Stolyar, and A. V. Rogachev, Int. J. Biol. Macromol. **164**, 3559 (2020).
[12] C. G. Chilom, B. Zorilă, M. Bacalum, M. Bălăşoiu, R. Yaroslavtsev, S. V. Stolyar, and S. Tyutyunnicov, Chem. Phys. Lipids **226**, 104851 (2020).
[13] S. V. Stolyar, L. A. Chekanova, R. N. Yaroslavtsev, S. V. Komogortsev, Y. V. Gerasimova, O. A. Bayukov, M. N. Volochaev, R. S. Iskhakov, I. V. Garanzha, O. S. Kolovskaya, M. S. Bairmani, and T. N. Zamay, J. Phys. Conf. Ser. **1399**, 022026 (2019).
[14] M. Ozaslan, I. D. Karagoz, I. H. Kilic, and M. E. Guldur, Afr. J. Biotechnol. **10**, 2375 (2011).
[15] D. A. Balaev, A. A. Krasikov, A. A. Dubrovskii, O. A. Bayukov, S. V. Stolyar, R. S. Iskhakov, V. P. Ladygina, and R. N. Yaroslavtsev, Tech. Phys. Lett. **41**, 705 (2015).
[16] D. A. Balaev, A. A. Krasikov, A. A. Dubrovskiy, S. I. Popkov, S. V. Stolyar, O. A. Bayukov, R. S. Iskhakov, V. P. Ladygina, and R. N. Yaroslavtsev, J. Magn. Magn. Mater. **410**, 171 (2016).
[17] E. Murad and U. Schwertmann, Am. Mineral. **65**, 1044 (1980).
[18] A. F. Vanin, Physics-Uspekhi **43**, 415 (2000).
[19] J. Bustamante, G. Bersier, R. A. Badin, C. Cymeryng, A. Parodi, and A. Boveris, Nitric Oxide **6**, 333 (2002).
[20] M. Jaiswal, N. F. LaRusso, L. J. Burgart, and G. J. Gores, Cancer Res **60**, 184 (2000).
[21] Y. Li, G. Chen, J. Zhao, X. Nie, C. Wan, J. Liu, Z. Duan, and G. Xu, Toxicology **312**, 132 (2013).
[22] J. Green, M. D. Rolfe, and L. J. Smith, Virulence **5**, 794 (2014).